



1 **Challenges in flood modelling over data scarce regions: how to exploit**
2 **globally available soil moisture products to estimate antecedent soil wetness**
3 **conditions in Morocco**

4
5 El Mahdi El Khalki¹, Yves Trambly^{2,*}, Christian Massari³, Luca Brocca³, Mohamed El Mehdi Saidi¹

6
7 ¹ Geosciences and Environment Laboratory, Cadi Ayyad University, Marrakesh, 40000, Morocco

8 ² HydroSciences Montpellier (Univ. Montpellier, CNRS, IRD), Montpellier, 34000, France

9 ³ Research Institute for Geo-Hydrological Protection, National Research Council, Perugia, 06100,
10 Italy

11 * Correspondence to: Yves Trambly (yves.trambly@ird.fr)

12
13 **Abstract:** The Mediterranean region is characterized by intense rainfall events giving rise to
14 devastating floods. In Maghreb countries such as Morocco, there is a strong need for forecasting
15 systems to reduce the impacts of floods. The development of such a system in the case of ungauged
16 catchments is complicated but remote sensing products could overcome the lack of in-situ
17 measurements. The soil moisture content can strongly modulate the magnitude of flood events and
18 consequently is a crucial parameter to take into account for flood modeling. In this study, different
19 soil moisture products (ESA-CCI, SMOS, SMOS-IC, ASCAT satellite products and ERA5
20 reanalysis) are compared to in-situ measurements and one continuous soil moisture accounting
21 (SMA) model for basins located in the High-Atlas Mountains, upstream of the city of Marrakech.
22 The results show that the SMOS-IC satellite product and the ERA5 reanalysis are best correlated
23 with observed soil moisture and with the SMA model outputs. The different soil moisture datasets
24 were also compared to estimate the initial soil moisture condition for an event-based hydrological
25 model based on the Soil Conservation Service Curve Number (SCS-CN). The ASCAT, SMOS-IC
26 and ERA5 products performed equally well in validation to simulate floods, outperforming daily in
27 situ soil moisture measurements that may not be representative of the whole catchment soil moisture
28 conditions. The results also indicated that the daily time step may not fully represent the saturation
29 state before a flood event, due to the rapid decay of soil moisture after rainfall in these semi-arid
30 environments. Indeed, at the hourly time step, ERA5 and in-situ measurements were found to better
31 represent the initial soil moisture conditions of the SCS-CN model by comparison with the daily time
32 step. The results of this work could be used to implement efficient flood modelling and forecasting
33 systems in semi-arid regions where soil moisture measurements are lacking.

34
35 **Keywords:** Soil moisture, floods, Morocco, ERA5, Rheraya, Issyl, High Atlas

36



37 **1 Introduction**

38

39 The Mediterranean region is characterized by intense rainfall events generating floods with a very
40 short response time (Gaume et al., 2004; Merheb et al., 2016; Trambly et al., 2011). The socio-
41 economic consequences of these floods are very important in terms of fatalities or damages to the
42 infrastructures in particular for Southern countries (Vinet et al., 2016). This highlights the need for
43 forecasting systems to reduce the impacts of floods. Unfortunately, the development of such systems is
44 very complicated in the case of ungauged catchments (Creutin and Borga, 2003) such as in North
45 Africa and requires remote sensing products to overcome the lack of in situ measurements.
46 Furthermore, while several studies have been focused on northern Mediterranean catchments for flood
47 modelling, only a few studies are available on southern basins, yet those probably the most vulnerable
48 to floods.

49

50 The Moroccan catchments are exposed to intense flash floods, such as the event of August 17, 1995 in
51 the Ourika river where the max discharge reached in 45 minutes a peak discharge of 1030 m³/s
52 causing extensive damages and more than 200 casualties (Saidi et al., 2003). Few studies have been
53 carried out in Morocco to minimize the impact of floods by improving the forecasting systems, either
54 by event-based modeling of floods (El Alaoui El Fels et al., 2017; Boumenni et al., 2017; El Khalki et
55 al., 2018) or by hydro-geomorphological approaches (Bennani et al., 2019) to identify the areas at risk
56 of flooding. The severity of floods in these semi-arid regions is controlled by several factors including
57 precipitation intensity, soil permeability, steep slopes and soil moisture content at the beginning of
58 event (El Khalki et al., 2018; Trambly et al., 2012). In Mediterranean regions, the soil moisture
59 content varies between events and is known to strongly modulate the magnitude of floods (Brocca et
60 al., 2017; Tuttle and Salvucci, 2014) and particularly to be useful for flood modeling and forecasting
61 systems (Brocca et al., 2011; El Khalki et al., 2018; Koster et al., 2009; Marchandise and Viel, 2010;
62 Trambly et al., 2012). However, studies in North African basins are lacking to document the rainfall-
63 runoff relationship with soil moisture during floods (Merheb et al., 2016).

64

65 In most Mediterranean regions and particularly in North Africa, only a few measurements of soil
66 moisture are available. To represent spatial variability, several measurement at different locations are
67 needed due to the potentially large spatial variability of soil moisture for a wide range of scales
68 (Massari et al., 2014; Schulte et al., 2005; Western and Blöschl, n.d.). However, even the in-situ data
69 may not represent the spatial variability over a very wide area in the case of large basins. On the
70 contrary, satellite soil moisture products provide coverage of the earth's surface by microwave sensors.
71 There are two types of microwave sensors, active and passive, noting: 1) The Advanced Scatterometer
72 (ASCAT) soil moisture product is on board MetOp with good radiometric accuracy and stability. This
73 product provides a spatial resolution of 25 km with a temporal resolution of 1 day since January 2007



74 (Wagner et al., 2013). 2) The Soil Moisture and Ocean Salinity Mission (SMOS) product, which
75 begins in January 2010 with a spatial resolution of 50km (Kerr et al., 2012). The improvement of the
76 robustness of satellite soil moisture products can be achieved by merging passive and active
77 microwave sensors as initiated and distributed by ESA-CCI (European Space Agency Climate Change
78 Initiative) (Liu et al., 2011) providing data from 1978 to 2018. However, remote sensing products
79 might suffer from several problems in complex topography or very dense vegetation and snow cover
80 (Brocca et al., 2017). For this reason and before any use the data, it is necessary to validate them (Al-
81 Yaari et al., 2014; Van doninck et al., 2012; Ochsner et al., 2013), either by in-situ measurements, if
82 they exist, or by using Soil Moisture Accounting models (Javelle et al., 2010; Trambly et al., 2012) to
83 simulate soil moisture in the ungauged basins.

84

85 In this context, with an increasing number of satellite products becoming available to estimate soil
86 moisture, clear guidelines and recommendations about the most suitable products to estimate the initial
87 soil moisture content prior to floods are lacking for the semi-arid basins of North Africa. The purpose
88 of this study is to compare different satellite soil moisture products with in-situ soil moisture
89 measurements and the recently developed ERA5 reanalysis to estimate the initial soil moisture before
90 flood events. The goal is to identify the best products to be used for flood modelling that could
91 improve forecasting systems. This comparison is performed for two basins representative of medium-
92 size catchments of North Africa that are the most sensitive to flash flood events. The validation of the
93 different soil moisture products is made with a Soil Moisture Accounting (SMA) model, to test the
94 capabilities of the different soil moisture products for the sake of estimating the initial conditions for
95 an event-based hydrological model for floods. The paper is organized as follow: In section 2, an
96 overview of the study area and all used data (hydro-meteorological and soil moisture products).
97 Section 3 explains the methods adopted in this paper. Section 4 presents the results. The conclusion
98 and perspectives are given in the last section.

99

100 **2 Study area and data**

101

102 **2.1 Rheraya and Issyl catchments**

103

104 The Rheraya research catchment (Jarlan et al., 2015) is located in the Moroccan High Atlas Mountains
105 (Figure 1) with an altitude ranging from 1027 to 4167m and an area of 225km². The climate in the
106 basin is semi-arid, strongly influenced by altitude, with a mean annual precipitation of 732mm,
107 including 30% as snow in altitudes above 2000m (Boudhar et al., 2009). The geology is characterized
108 by volcanic formations that are considered impermeable in the highest elevation areas, while the
109 lowest elevation areas are made of granites with clays and marls. In the highest elevation areas very
110 steep slopes are found with an average of 19% (Chaponnière et al., 2008). The vegetation cover is only



111 located in the lowest areas with a concentration of cultivated areas found along the river channel.
112 These natural conditions favor runoff generation. There is very low human disturbance for runoff, with
113 only some local water uptake in the lower part of the river.

114

115 The Issyl basin (Figure 1) is located in the foothills of the Moroccan High Atlas Mountains with an
116 altitude ranging from 632 to 2300m, an area of 160 km², and a mean annual precipitation of 666mm. It
117 is an ephemeral river with discharge occurring only after rainfall events. The climate is semi-arid to
118 arid and the downstream part of the basin reaches the city of Marrakech. The geological formations in
119 this downstream are alluvial conglomerates that are relatively permeable. The upstream of the basin
120 consists of clays and calcareous marl. The basin area includes agricultural activities that are irrigated
121 in the downstream part of the basin. The irrigation comes from *seguias*, earthen-made channels that
122 traditionally draw their water supply from the river itself, by building small diverting dams on the side
123 of the river (Pérennès, 1994). The *seguias* channels are usually filled up during floods, and water is
124 distributed to the neighboring agricultural parcels. The map on the *seguias* in the Issyl basin can be
125 seen in Figure 1, covering the northern part of the basin. The system is unmonitored and in a context
126 of high evaporation rates the portion of runoff diverted from the stream is not quantified. Due to the
127 temporary nature of *seguias*, they can be partially destroyed during large floods and consequently their
128 hydraulic properties and the amount of water collected can be modified over time.

129

130 **2.2 Hydro-meteorological data**

131

132 In the Rheraya basin, we used 8 rainfall stations, 5 of them from the data network of the Joint
133 International Laboratory Télédétection et Ressources en Eau en Méditerranée semi- Aride ‘‘LMI
134 TREMA’’ (Jarlan et al., 2015; Khabba et al., 2013) and the remaining ones from the Tensift Hydraulic
135 Basin Agency. The data is covering from 2008 to 2016. For the Issyl basin, only 2 rainfall stations are
136 available from the Tensift Hydraulic Basin Agency, covering the years from 2010 to 2015. In this type
137 of basin, the spatial variability of rainfall is very important (Chaponnière et al., 2008). The
138 hydrometric data was provided by radar installed in each basin’s outlet. The data is covering only the
139 year 2014 for Rheraya, since the sensor was installed at the end of 2013, and the years 2010 to 2015
140 for Issyl. The discharge data is provided with a time step of 10min converted into hourly time step as
141 for rainfall.

142

143 The discharge data is missing in some events that are not selected. For this reason we considered only
144 the events with complete discharge data. Some of the flood events considered in this study (Table 1)
145 occurred in winter season, where rainfall can be in the form of snow above 2000m elevation.
146 According to El khalki et al.(2018) the snow doesn’t contribute to runoff during winter season in the
147 Rheraya basin, where only 17% of basin area is occupied by snow. The runoff coefficients calculated



148 for each selected events are ranging from 13.1 to 34.1% for Rheraya and from 1.2 to 7.2% for Issyl.
149 This indicates the important role of initial conditions in both basins, with a much higher infiltration
150 capacity in the Issyl basin in addition to potential water loss due to irrigation. We used 5 temperature
151 stations located in the Rheraya basin and one temperature station located in the Issyl basin with an
152 hourly time step to calculate the average temperature over each basin, ranging from 2008 to 2016. This
153 data enabled us to calculate potential evapotranspiration (PET) with Oudin formula (Oudin et al.,
154 2005) requiring temperature only.

155

156 **2.3 Soil moisture data**

157

158 We used 7 different types of soil moisture data over the Rheraya basin and 6 types in the Issyl basin
159 due to the absence of measurements in this basin. Covering the same period of rainfall data mentioned
160 in the 2.3 section, we used:

- 161 1. In-situ measurement with three Thetaprobles at 5cm and 30cm depth in the Rheraya basin,
162 located at the SMPR7 station (Figure 1).
- 163 2. Simulated soil moisture from a Soil Moisture Accounting model (SMA)
- 164 3. ASCAT satellite soil moisture
- 165 4. SMOS satellite soil moisture
- 166 5. SMOS-IC satellite soil moisture
- 167 6. ESA-CCI satellite soil moisture
- 168 7. ERA5 reanalysis soil moisture

169

170 **2.3.1 In-situ measurements**

171

172 Soil moisture measurements are available at one location with three Thetaprobles at two different
173 depths (5cm and 30cm). In this study we used Thetaprobles with 5cm depth, which is comparable with
174 the depths of satellite products (Massari et al., 2014). The site is located in Rheraya basin, with an
175 altitude of 2030m and a slope of 30% (Figure 1). The data is covering the time period from 2013 to
176 2016, with 30min time step converted to daily time step.

177

178 **2.3.2 Soil moisture accounting model**

179

180 The SMA is a continuous Soil Moisture Accounting model that can be used in the absence of soil
181 moisture data to represent the degree of saturation for flood modeling (Anctil et al., 2004; Trambly et
182 al., 2012). In this study, a simplified version of the SMA model is used, adopting the same approach
183 used by Trambly et al. (2012) and Javelle et al. (2010). The SMA calculates the level of the soil
184 reservoir (S/A), ranging between 0 and 1, by calibrating its single parameter, A , which represents the



185 reservoir capacity. An interpolated daily rainfall dataset created by the Inverse Distance method and
186 evapotranspiration data computed from daily maximum and minimum temperature with the
187 Hargreaves-Samani equation (Hargreaves and Samani, 1982) are used as inputs to the SMA model.

188

189 **2.3.3 Soil moisture products**

190

191 In this study we used three different types of satellite products and a Reanalysis product: an active
192 product (ASCAT), two variants of a passive product (SMOS and SMOS-IC), a product that combines
193 the two active and passive products (ESA-CCI) and ERA5 product:

194

- 195 1. The Advanced SCATterometer (ASCAT) is a Soil Moisture product, onboard Metop-A
196 and Metop-B and a Metop-C satellite is a C-band (5.255 GHz) scatterometer onboard the
197 Metop satellite series. It has a spatial sampling of 12.5 km and 1 to 2 observations per day
198 (Wagner et al., 2013). The SM product was provided within the EUMETSAT project
199 (<http://hsaf.meteoam.it/>) denoted as H115.
- 200 2. The Soil Moisture and Ocean Salinity (SMOS) mission is a radiometer operating at L
201 band (1.4 GHz), providing Soil Moisture data with ~50km as spatial sampling and 1
202 observation per 2/3 days (Kerr et al., 2001). Centre Aval de Traitement des Données
203 SMOS (CATDS, <https://www.catds.fr/>) provided the version RE04 (level3) for this study.
204 This version is gridded on the 25km EASEv2 grid.
- 205 3. The Soil Moisture and Ocean Salinity INRA-CESBIO (SMOS-IC) is an algorithm
206 designed by Insitut National de la Recherche Agronomique (INRA) and Centre d'Etudes
207 Spatiales de la Biosphère (CESBIO) for a global retrieval of Soil Moisture and L-VOD.
208 Two parameters of inversion of the L-MED model are used in the SMOS-IC (Wigneron
209 et al., 2007) with a consideration of the pixel as homogeneous. This version is 105 and
210 has a spatial sampling of 25km with EASEv2 Grid (Fernandez-Moran et al., 2017).
- 211 4. The ESA-CCI soil moisture product (<http://www.esa-soilmoisture-cci.org/>) regroups
212 active and passive microwave sensors to measure soil moisture, giving three type of
213 products: Active, Passive and Combined (Active + Passive). In this paper, the ESA-CCI
214 V4.5 – Combined product is used (Dorigo et al., 2017; Gruber et al., 2017, 2019). The
215 product has been validated to be useful by 600 ground-based measurement points around
216 the globe (Dorigo et al., 2015), as well as it was compared with ERA-Interim products
217 (Albergel et al., 2013). In the field of hydrological modeling, several global studies have
218 used the ESA-CCI product to initiate the hydrological model (Dorigo et al., 2012, 2015;
219 Massari et al., 2014) at the scale of Morocco (El Khalki et al., 2018). We extracted for
220 each basin the pixel that corresponds to it.



221 5. ERA5 (Copernicus Climate Change Service (C3S), 2017) developed by European Centre
222 for Medium-Range Weather Forecasts (ECMWF), it is the latest version of atmospheric
223 reanalysis available for public since February 2019. The ERA5 replaced ERA-Interim
224 with improvement at different scales, particularly, a higher spatial and temporal
225 resolution, and a better global balance of precipitation and evaporation. The spatial
226 resolution is 31km instead of 79km, hourly resolution is used instead of 6 hours, and the
227 covered period will be extended to 1950 in future. The ERA5 product was applied in
228 some recent studies in hydro-climatic field (Albergel et al., 2018; Hwang et al., 2019;
229 Mahto and Mishra, 2019; Olauson, 2018). We selected the volumetric soil water of the
230 first soil layer. This new product is tested in our study for the first time in Morocco. An
231 alternative dataset, ERA5-Land using an improved land-surface scheme with a spatial
232 resolution of 10km, was also tested, providing the same results as ERA5 since there is a
233 strong correlation between soil moisture simulated by the two products.

234

235 **3 Methods**

236

237 **3.1 Evaluation of different soil moisture datasets**

238

239 In-situ data preparation consists of averaging the 5cm depth probes in order to get a single value to
240 work with and take into account the plot-scale variability of the measurements. This data is considered
241 as a reference for soil moisture data in the Rheraya basin, so that all the other soil moisture products
242 are compared to it. The different soil moisture products are compared to the observed soil moisture
243 over the entire period and also on a seasonal basis.

244

245 The SMA model is used to represent the soil moisture aggregated at the catchment scale. The rationale
246 behind the use of such model here is that continuous rainfall and temperature series are often available
247 in monitored catchments, unlike soil moisture, and a calibrated SMA model can sometimes palliate the
248 lack of soil moisture measurements (Tramblay et al., 2012). For the SMA model, the A parameter,
249 representing the soil water holding capacity, is calibrated to obtain the best correlation between
250 observed and simulated soil moisture (S/A). The calibration with observed data can only be performed
251 in the Rheraya basin where soil moisture is measured. In addition to this calibration, other values of A,
252 ranging between 1 and 1000, are tested in the SMA model to maximize the correlations with the
253 different soil moisture products. The choice of this approach is to check if there are any possible
254 uncertainties that can be related to the in-situ soil moisture measurements, located on a steep slope plot
255 that may not fully represent the average soil moisture conditions over the whole basin. In the case of
256 the Issyl basin, since there is no observed soil moisture data, the model is run for a range of different



257 values of the A parameter. The best value of the A parameter is selected as the one yielding the best
258 correlations with the different satellite products.

259

260 The values from ASCAT and SMA are given in percentage (values are ranging between 0 and 1) while
261 SMOS, SMOS-IC, ERA5, ESA-CCI and observations are in $\text{m}^3 \text{m}^{-3}$. To allow a comparison for all soil
262 moisture datasets a rescaling procedure is needed. Before applying the rescaling procedure, according
263 to Albergel et al. (2010), a 95% confidence interval is chosen to define the higher and lower values to
264 exclude any abnormal outliers using equation 1 and 2. The resulted data is then rescaled to their own
265 maximum and minimum values considering the whole period using the equation 3. The issue in the
266 validation of satellite soil moisture products and reanalysis product with in-situ measurements is the
267 spatial resolution (Jackson et al., 2010). Several studies mentioned that, in the case of the temporal
268 stability introduced by Vachaud et al. (1985), one in-situ measurement point can represent the soil
269 moisture condition of a larger area (Brocca et al., 2009b, 2010; Loew and Mauser, 2008; Loew and
270 Schlenz, 2011; Martínez-Fernández and Ceballos, 2005; Miralles et al., 2010; Wagner et al., 2008).
271 According to (Massari et al., 2015), the coarse satellite observations can be beneficial for small basins,
272 in the case if the in-situ observation falls in the satellite product pixel. This means that the in-situ
273 measurements can represent a good benchmark (Liu et al., 2011). In this study we considered the in-
274 situ measurement as a benchmark to validate different soil moisture products.

275

$$Up_{SM} = \mu_{SM} + 1.96\sigma_{SM}, \quad (1)$$

$$Low_{SM} = \mu_{SM} - 1.96\sigma_{SM}, \quad (2)$$

276 Where Up_{SM} and Low_{SM} are the limits of the confidence interval (the upper and the lower 95%)

277

$$SM = \frac{SM - Low_{SM}}{Low_{SM} - Up_{SM}}, \quad (3)$$

278

279 **3.2 Extended collocation analysis:**

280

281 An alternative technique to validate soil moisture products when ground truth is missing is the use of
282 Triple Collocation (TC) analysis (Gruber et al. 2016b). TC analysis requires the availability of three
283 datasets with mutually independent errors and linear additive error model between the measurement
284 systems and the unknown truth:

285

$$X = \alpha + \beta S + \varepsilon, \quad (4)$$

286

287 where X is the soil moisture estimate, S is the true soil moisture, α and β are additive and
288 multiplicative biases, respectively. Eventually, ε is the zero-mean random error.



289

290 To build such a triplet, satellite and ground-based datasets can be combined with modeled soil
 291 moisture fields from reanalysis (e.g., ERA5). The reanalysis datasets ingest a number of satellite,
 292 atmospheric and ground observations which can potentially undermine their independence with
 293 respect to other members of the triplets. This creates doubts about the satisfaction of the null cross-
 294 correlation assumptions required to apply TC (Stoffelen, 1998). In a preliminary analysis (not shown),
 295 we used TC to characterize the error variance of the different soil moisture datasets by using different
 296 triplet combinations of the products. However, we observed substantial differences among the selected
 297 triplets likely due to error co-dependence. Based on that, we assumed the existence of non-null error
 298 cross correlation for the selected triplets (e.g. ERA5, SMOS and ASCAT).

299

300 When more than three products are available (i.e., N), the error can be estimated using an Extended
 301 Collocation (EC) approach (Gruber et al. 2016). The same assumptions for TC also apply for EC, but
 302 the number (N >3) datasets constitutes an over-constrained system, allowing the designation of N-3
 303 non-zero error covariance terms which can be estimated with a least-squares solution (Pierdicca et al.
 304 2015). Therefore, the zero TC assumption can be relaxed to allow non-zero correlation among N-3
 305 data product pairs. For N = 4, the X, Y, Z, W measurement systems and assuming that non-zero EC
 306 exists only between X and Y, the least-squares solution for the QC problem is given by:

307

$$M = \begin{bmatrix} \sigma_X^2 \\ \sigma_Y^2 \\ \sigma_Z^2 \\ \sigma_W^2 \\ \sigma_{XY} \\ \sigma_{XZ}\sigma_{XW}/\sigma_{ZW} \\ \sigma_{YZ}\sigma_{YW}/\sigma_{ZW} \\ \sigma_{XZ}\sigma_{ZW}/\sigma_{XW} \\ \sigma_{YZ}\sigma_{ZW}/\sigma_{YW} \\ \sigma_{XW}\sigma_{ZW}/\sigma_{XZ} \\ \sigma_{YW}\sigma_{ZW}/\sigma_{YZ} \\ \sigma_{XZ}\sigma_{YW}/\sigma_{ZW} \\ \sigma_{XW}\sigma_{YZ}/\sigma_{ZW} \end{bmatrix} A = \begin{bmatrix} 1000010000 \\ 0100001000 \\ 0010000100 \\ 0001000010 \\ 0000100001 \\ 1000000000 \\ 0100000000 \\ 0010000000 \\ 0010000000 \\ 0001000000 \\ 0001000000 \\ 0000100000 \\ 0000100000 \end{bmatrix} S = \begin{bmatrix} \beta_X^2 \sigma_T^2 \\ \beta_Y^2 \sigma_T^2 \\ \beta_Z^2 \sigma_T^2 \\ \beta_W^2 \sigma_T^2 \\ \beta_X \beta_Y \sigma_T^2 \\ \sigma_{\epsilon_X}^2 \\ \sigma_{\epsilon_Y}^2 \\ \sigma_{\epsilon_Z}^2 \\ \sigma_{\epsilon_W}^2 \\ \sigma_{\epsilon_X \epsilon_Y} \end{bmatrix} \quad (5)$$

308

309 where σ_T^2 is the true soil moisture variance, σ_{ϵ}^2 is the variance of the random error, and $\sigma_{(\epsilon_X \epsilon_Y)}$
 310 is the error covariance between X and Y.

311

312 And the least squares solution for the parameters in S is given as:

313

$$\hat{S} = (A^T A)^{-1} A^T M, \quad (6)$$

314



315 Which provide the error variance of each dataset as long as the error covariance terms. More details on
316 the method and its mathematical derivation can be found in Gruber et al. (2016). The error variance
317 provided by EC can also be expressed in normalised form as Signal-to-Noise Ratio (SNR). This
318 overcomes the dependency on the chosen scaling reference and allows to compare the error variances
319 between the data sets. SNR is usually given in decibel, which can be easily interpreted: a value of zero
320 means that the signal variance is equal to the noise variance, and every 3dB increase(decrease) implies
321 a doubling (halving) of the signal variance compared to the noise variance. The SNR (expressed in
322 dB) can be computed using the following formulation:

323

$$SNR[db] = 10 \log \frac{\beta_i^2 \sigma_\theta^2}{MSE_i}, \quad (7)$$

324 with i, j in $[X, Y, Z]$ and $i \neq j$.

325

326 In some special cases, the MSE_i can become negative and the SNR cannot be expressed in dB
327 (logarithm of a negative number is undefined). The reason is that the relation of the covariances
328 between the data sets become larger than the actual signal variance (e.g. $\#XY \#XZ/\#Y Z > \#2X$),
329 which can be related numerical problems, wrong estimation of the covariances or a violation of the
330 underlying assumptions of the error model in general. In our study we used two different
331 configurations of the EC techniques. In particular, for the Issyl basin no in situ observations are
332 available so we used quadruple collocation analysis with quadruplets constructed with ASCAT,
333 SMOS, ERA5 and SMA and ASCAT, SMOS-IC, ERA5 and SMA. The choice of these quadruplets
334 was based on the assumption of non-zero correlation between SMOS products and ERA5 so in the
335 process we also estimated $\sigma_{(SMOS-ERA)}$ (not shown). Similarly, for Rheraya we applied the
336 methods by using five different datasets and assuming SMOS and ERA products and SMA and in situ
337 observations characterized by non-null error cross-correlations. For both basins we used either SMOS
338 or SMOS-IC in the configurations.

339

340 **3.3 Event-based hydrological model for floods**

341

342 In this study, we used the Soil Conservation Service Curve Number (SCS-CN) model for each basin,
343 implemented in the hydrologic Engineering System - Hydrologic Modeling System ‘‘HEC-HMS’’
344 software (US Army Corps of Engineers, 2015). This model is known by its widespread popularity and
345 to the simplicity of the application method (Miliani et al., 2011). SCS-CN is often used in the semi-
346 arid context (Brocca et al., 2009a; El Khalki et al., 2018; Trambly et al., 2010; Zema et al., 2017).
347 Our methodology is based on the use of SCS-CN model as a production function to compute net
348 rainfall, by manually calibrating the Curve Number parameter (CN), the value of CN is non-



349 dimensional ranging from 0 (dry) to 100 (wet). The potential maximum retention, S, is related to CN
 350 as follows:

351

$$S = \frac{25400}{CN} - 254, \quad (8)$$

352

353 The transformation of precipitation excess into runoff is provided by Clark Unit hydrograph model
 354 (transfer function). The calibration procedure is based on calibrating the Clark Unit hydrograph model
 355 parameters; Storage Coefficient (Sc) and Time of Concentration (Tc). The two functions (production
 356 and transfer) are calibrated separately to avoid the parameter dependence.

357

358 The validation procedure is based on two steps; first, testing the relationship between soil moisture
 359 data (In-situ, SMA, ERA5, ASCAT, SMOS, SMOS-IC and ESA-CCI), at two different timescales
 360 (daily and hourly) and the S parameter of the event-based model of all the flood events. The hourly
 361 time step concerns only the in-situ data and ERA5 by choosing the soil moisture state 1 hour before
 362 the starting time of rainfall for each event. Only the ERA5 product can be used in the Issyl basin at the
 363 hourly time step due to the absence of observed data. Then, the soil moisture products that are well
 364 correlated with S parameter are used to validate the model by calculating the S parameter from the
 365 linear equation obtained between soil moisture and S, using the leave-one-out resampling procedure;
 366 each event is successively removed and a new relationship between the remaining event is re-
 367 computed. The estimated S parameter for a given event is then used in the SCS-CN model in
 368 validation. For the Clark Unit Hydrograph model, the average of the Sc and the Tc parameters are used
 369 in validation.

370

371 The correlation coefficient of Pearson equation (9) and the Root Mean Square Deviation (RMSD)
 372 equation (10) are used to compare in-situ measurements and humidity modeled by SMA model and
 373 the different soil moisture products. For the evaluation of the flows simulated by the flood event
 374 model, we compared the simulated discharge with those observed using the efficiency coefficient of
 375 Nash-Sutcliffe (Ns) (Nash and Sutcliffe, 1970) equation (11) as well as through the bias on peak flow
 376 and on volume equation(12).

377

$$r = \frac{N \sum SM_{sat} SM_{In-situ} - (\sum SM_{sat})(\sum SM_{In-situ})}{\sqrt{[N \sum SM_{sat}^2 - (\sum SM_{sat})^2][N \sum SM_{In-situ}^2 - (\sum SM_{In-situ})^2]}}, \quad (9)$$

$$RMSD = \sqrt{\frac{\sum_{i=1}^n (SM_{In-situ} - SM_{sat})^2}{N}}, \quad (10)$$

$$Ns = 1 - \frac{\sum_{i=1}^n (Q_{obs,i} - Q_{sim,i})^2}{\sum_{i=1}^n (Q_{obs,i} - Q_{obs})^2}, \quad (11)$$



$$\text{BIAS}_Q = \frac{(Q_{\text{sim}} - Q_{\text{obs}})}{Q_{\text{obs}}}, \quad (12)$$

378

379 Where Q_{sim} is the simulated discharge, Q_{obs} is the observed discharge, $SM_{\text{In-situ}}$ is the in-situ
380 measurements of soil moisture, SM_{sat} is the soil moisture from satellite or reanalysis and N is the
381 number of values. The N s ranges between $-\infty$ and 1, the 1 value of N s indicates that the simulated
382 discharge perfectly match the observed hydrograph

383

384 4 Results and discussions

385

386 4.1 Relationship between satellite soil moisture data and in-situ measurements

387

388 The comparison between measured soil moisture at 5cm depth and the different products of soil
389 moisture show that the SMOS-IC and ERA5 provide the best correlations, with $r=0.76$ and $r=0.67$
390 respectively, but it should be noted that all the correlations with the different products are also
391 significant. Figure 2 shows that SMOS-IC and ERA5 reproduce dry periods well, whereas ERA5
392 reproduces well wet periods. This result is in accordance with the results of Massari et al. (2014) who
393 found that ERA-Land is well correlated with In-situ data. ASCAT product shows a correlation of
394 $r=0.43$ which is less than the correlation given in Albergel et al. (2010) who found r values ranging
395 from between 0.59 and 0.64, the lower correlation may be caused by the orography and the coarse
396 resolution. In fact, this results shows that the use of a combined product as ESA-CCI give an obvious
397 advances in term of r values than one single satellite soil moisture product (Ma et al., 2019; Zeng et
398 al., 2015). It should be noted that the soil moisture products have a different percentage of missing
399 data for ASCAT (0%), SMOS (18.7%), SMOS-IC (6.82%), ESA-CCI (46%) and observed soil
400 moisture (12%). The ESA-CCI showed an important percentage of missing values comparing to
401 ASCAT that is integrated in the ESA-CCI product. This due to the filter used in the ESA-CCI product
402 to ensure the data quality, more description can be found in (Dorigo et al., 2017).

403

404 4.2 Relationship between the SMA model outputs and soil moisture products

405

406 The best correlation between observed soil moisture and the soil moisture level (S/A) modeled by the
407 SMA model is obtained for $A=8\text{mm}$ with $r=0.86$. But it shows higher RMSD than observations
408 ($\text{RMSD}=0.23$) which is due to the overestimation of the wet periods (Figure 3). This can be related to
409 the averaging of rainfall data in the SMA model over the basin which could be higher than rainfall in
410 the soil moisture measurement site. It should be noted that the value of the A parameter is very small
411 by comparing to previous studies (Javelle et al., 2010; Trambly et al., 2012), indicating a much lower
412 soil storage capacity.



413

414 We correlated the SMA model output (for $A=8\text{mm}$) with the Satellite Products of Soil Moisture, and
415 the best correlations are found for SMOS-IC and ERA-5, with $r=0.74$ and $r=0.63$ respectively (Figure
416 4). Other values of A that maximize the correlations with the different soil moisture products have also
417 been tested. Optimal values of A are ranging from 1 mm with ASCAT (with $r=0.4$), 8 mm for SMOS
418 ($r=0.56$), SMOS-IC ($r=0.75$) and ESA-CCI ($r=0.55$) up to 16mm for ERA5 ($r=0.68$). Comparing the
419 Figure 2 and Figure 4 we notice that the soil moisture products better reproduce in-situ measurements
420 than modelled soil moisture with the SMA model, expect for ESA-CCI and SMOS. This improvement
421 is directly related to the SMA model performance, which overestimates soil moisture, and should be
422 compared to Figure 2 where ESA-CCI and SMOS products also overestimate in-situ measurements.

423

424 For the Issyl basin, the percentage of missing values is a bit lower than in the Rheraya and also
425 different between the satellite products: ASCAT (0%), SMOS (17.19%), SMOS-IC (9.1%) and ESA-
426 CCI (2.2%). As mentioned above, no observed soil moisture data is available in the Issyl basin to
427 calibrate the A parameter of the SMA model. Therefore, different values of A are tested to correlate
428 the SMA outputs with the different soil moisture datasets. Over all datasets, the value of A best
429 correlated to the majority of soil moisture products is 30mm. The best correlation is given by
430 $A=30\text{mm}$ with $r=0.78$, 0.82 and 0.79 for ASCAT, SMOS-IC and ESA-CCI respectively. As for SMOS
431 and ERA5, the best correlation is given for $A=40\text{mm}$ with $r=0.7$ and $A=60\text{mm}$ with $r=0.8$,
432 respectively. In order to choose a single value of A that represents the basin, we have considered
433 $A=30\text{mm}$, the optimal value yielding the best correlations with the different soil moisture products.
434 Figure 5 shows that the best correlation between satellite products and S/A is obtained with SMOS-IC
435 ($r=0.82$) and ESA-CCI ($r=0.79$). As observed over the Rheraya basin, the SMOS-IC and ERA5
436 products showed a good reproduction for dry periods with a better reproduction of wet periods with
437 ERA5, these results are similar to those of Ma et al. (2019) who found that SMOS-IC performs well in
438 arid zones with a median r value of 0.6. Overall, the higher value for the A parameter found for this
439 basin is coherent with the fact that this basin is located in a plain area with a much higher soil moisture
440 storage capacity than in the mountainous Rheraya basin.

441

442 4.3. Comparison of soil moisture datasets by seasons

443

444 Seasonal evaluation of satellite soil moisture and reanalysis data shows for the Rheraya basin that
445 during the summer season there are low correlations (average $r=0.34$) for all the products which is
446 possibly due to very low precipitation amounts mostly as localized convective precipitation (Albergel
447 et al., 2010). On the contrary, better performance are obtained with the SMA model ($r=0.59$) that
448 considers catchment-scale precipitations. Better correlations are obtained in fall with an average of
449 $r=0.61$ and 0.58 for the in-situ data and SMA respectively (Table 2). In the winter we found a poor



450 correlation using SMOS and ESA-CCI that can be related to the important percentage of missing
451 values. For the Issyl watershed, the satellite products show good correlations with the SMA model
452 outputs (on average $r=0.76$) except for the SMOS product especially in winter. We also notice a trend
453 of improving correlations by moving from winter to autumn with a similarity between spring and
454 autumn, which is not the case in the Rheraya basin, probably because of different precipitation
455 patterns. The ERA5 overall product shows good correlations for most seasons.

456

457 **4.4 Extended collocation analysis**

458

459 Table 3 shows the results obtained for the two basins and two configurations. For Issyl, it can be seen
460 that SMOS-IC is the best performing product with SNR much larger 3DB, followed by ASCAT and
461 SMA. Conversely ERA5 and SMOS are suboptimal having noise variance similar to the signal
462 variance. For Rheraya SMOS-IC is the only product providing $SNR>3DB$ followed by SMOS and
463 ERA5 which are however are still suboptimal. Poor results are found for both SMA, in situ and
464 ASCAT in this catchment. Overall, the results of this complementary analysis confirm the findings of
465 previous sections.

466

467 **4.5 Calibration of the event-based hydrological model**

468

469 Calibration results (Table 4) on the individual flood events of Table 1 show that the difference
470 between the values of the potential maximum soil moisture retention (S) of each basin is very
471 important with larger values for the Issyl basin where the soil depth is prominent. We noticed that the
472 temporal variability of soil moisture can be important between two successive events like the events of
473 02/04/2012 and 05/04/2012 for the Issyl basin. The SCS-CN model reproduces well the floods of the
474 Rheraya basin with average N_s of 0.67 and bias on runoff peak ($BIAS_Q$) of 4% (Table 3). As shown on
475 Figure 6, the SCS-CN model in calibration is able to reproduce the shape of the different flood events
476 even for the most complex ones (21/04/2014 and 22/11/2014). Similarly, for the Issyl basin the SCS-
477 CN model gives good results with average N_s of 0.66 and an average bias on runoff peak of 6.93%.
478 Figure 7 shows the simulated hydrographs which are in good agreement with the observations. The
479 lower N_s coefficients obtained for the 23/01/2014 event in the Rheraya and for the 03/04/2011 and
480 28/09/2012 events in the Issyl basin are caused by a slight shift in the hydrograph probably due to a
481 time lag in instantaneous precipitation measurements. For the Clark Unit Hydrograph model, the
482 averages of calibrated T_c and S_c parameters are considered for validation ($S_c = 1.42$ and 2.54 hours
483 and $T_c = 2.85$ and 3.64 hours for Rheraya and Issyl respectively).

484

485 The S parameters of the hydrological models, for the two basins, are then compared to the soil
486 moisture products. For the Rheraya basin, there are significant correlations of the S parameter with in-



487 situ soil moisture data, ERA5 and SMOS-IC (Table 5). The correlations using observed soil moisture,
488 ESA-CCI and SMOS data can be computed with only 8 and 6 events respectively, due to the presence
489 of missing values. The time step of the soil moisture data in the Rheraya basin seems to play a key role
490 in the representation of soil moisture conditions. Indeed, the daily time step shows a weakness to
491 effectively represent the antecedent soil moisture conditions in the SCS model, which indicates the
492 rapid change of soil moisture content in such a semi-arid mountainous basin. For the Issyl basin, ESA-
493 CCI is the only satellite product that is significantly correlated to the S parameter at the daily time
494 step. The ERA5 product is also significantly correlated with the S parameter but at the hourly time
495 step. The daily output of the SMA model is also able to estimate the initial condition of the model for
496 the Issyl basin, with a correlation of -0.69 with S. Interestingly, the SMA model does not provide a
497 good performance in the Rheraya basin. It can be due to the fact that in such a mountainous basin,
498 there is a strong spatial variability of rainfall and it is difficult to obtain reliable precipitation estimates
499 for continuous simulations (Chapponiere et al., 2005).

500

501 **4.6 Validation of the event-based hydrological model**

502

503 The validation of the event-based hydrological model is performed on the events of Rheraya and Issyl
504 using only the soil moisture datasets that show relatively good correlations with the initial condition
505 (S) of the model from Table 6. These products include SMOS-IC, ERA5 and observed soil moisture
506 for the Rheraya, and ESA-CCI, ERA5, SMOS and SMA for Issyl. The validation of the event-based
507 model is performed with S calculated from the linear equation obtained from the correlation analysis
508 between the different soil moisture products and the calibrated parameter S. The validation results
509 show that for the Rheraya basin the events are well validated using both daily (Figure 6) and hourly
510 (Figure 7) time step of soil moisture products. The best validation result at the daily time step is
511 obtained with SMOS-IC with an average N_s of 0.58 for all events (median $N_s = 0.63$). This result
512 should be compared with the results found in the previous sections where SMOS-IC showed the best
513 correlations with observed soil moisture. ASCAT and ERA5 show similar results in term of average
514 N_s (~0.45). On the contrary, the daily observed soil moisture shows a lower performance with an
515 average N_s of 0.25 (median $N_s = 0.49$). The hourly time step enhanced the performance of the model,
516 with an average N_s using the ERA5 product of 0.64 (median $N_s = 0.73$) and also a better performance
517 with the hourly in-situ data with mean $N_s = 0.54$ (median $N_s = 0.61$). These results show that the
518 hourly time step better represents the saturation content before the flood events in this basin. For the
519 Issyl, the validation results are quite different (Figure 8). For only 5 events (the 03/04/2011,
520 02/05/2011, 19/05/2011, 05/04/2012 and 25/03/2015) the event-based model can be validated using
521 the ERA5 hourly data with an average N_s coefficient of 0.46, while for all other events and with
522 different soil moisture products the N_s coefficients are negative and the hydrographs not adequately
523 reproduced. These validation results should be put in perspective with the fact that the Issyl basin has a



524 land use characterized by agricultural activities with possible large water uptake in the diver channel
525 during floods for irrigation. Some simple methods to compensate for the water losses due to irrigation,
526 such as the application of a varying percentage of runoff added to the observed discharge to
527 compensate the part of water lost for irrigation, have been tested but with no improvement of the
528 results. This is probably because the quantity taken for irrigation is not constant from one event to
529 another depending on the farmer needs, as shown by field surveys, and this amount may also depend
530 on discharge thresholds.

531

532 **5 Conclusions**

533

534 This study performed an evaluation of different soil moisture products (ASCAT, ESA-CCI, SMOS,
535 SMOS-IC and ERA5) using in-situ measurements and a Soil Moisture Accounting model (SMA) over
536 two basins located in the Moroccan High Atlas in order to estimate the initial soil moisture conditions
537 before flood events. There is a knowledge gap on the evaluation of soil moisture products in North
538 Africa (Jiang and Wang, 2019) that the present study aimed to fill. The results indicated that the
539 SMOS-IC product is well correlated with both the in-situ soil moisture measurements and simulated
540 soil moisture from the SMA model over the two basins. Beside satellite products, the new ERA5
541 reanalysis reproduced also well the in-situ measurements over the mountainous basin, which indicates
542 the robustness of this product to estimate soil moisture in these semi-arid environments. The seasonal
543 analysis showed increasing correlations coefficients, from winter to autumn, for all the soil moisture
544 products when compared to observations, which encourages the use of these remote sensing products
545 for flood forecasting because the majority of events occur in autumn and early winter in these regions
546 (El Khalki et al., 2018). The extended collocation analysis show coherent results with the correlation
547 results with the SMOS-IC providing the best results for the Issyl and Rheraya basins. One of the main
548 finding of the present study is that different products, in particular SMOS-IC, ASCAT and ERA5, are
549 efficient to estimate the initial soil moisture conditions in an event-based hydrological model, that
550 could improve the forecasting capability in data-scare environments.

551

552 This study also showed that the hourly temporal resolution for soil moisture may provide a better
553 estimate of the initial soil moisture conditions for both basins. Indeed, the use of hourly in-situ soil
554 moisture measurements and ERA5 provided better performance to estimate the initial condition of the
555 hydrological model. These results indicate that the temporal variability of soil moisture in these semi-
556 arid basins under high evapotranspiration rates can be very important causing a quick decay of soil
557 moisture following a rainfall event. For this type of basin or others under even more arid conditions,
558 the use of soil moisture products with an hourly temporal resolution could be required to estimate with
559 accuracy the soil moisture content prior to flood events. This constitute a research challenge to
560 monitor soil moisture at the sub-daily timescale without ground measurements, since most remote



561 sensing products at present are not available at the hourly time step. As shown by this study,
562 atmospheric reanalysis coupled with a land surface model, such as ERA5, could provide a valuable
563 alternative, in particular since the resolution of these products is constantly improving along with a
564 more realistic representation of water balance.

565

566 For the catchment that is the most influenced by agricultural activities, the Issyl basin located nearby
567 Marrakech, the water uptake for irrigation made difficult the validation of the hydrological model. The
568 model overestimates runoff for some flood events, since the water uptake during floods from the river
569 channel by small artisanal structures is not monitored and thus cannot be represented in the
570 hydrological model. This example show the difficulty in the implementation of a flood forecasting
571 system in such basin without a good knowledge on the human influences on river discharge. This
572 situation is not a particular case but deemed common in semi-arid areas where rivers with a high risk
573 of flooding are also a substantial water resource for agriculture. Therefore, as shown by our results, a
574 hydrological model that is not accounting for water use and irrigation may not be efficient at
575 reproducing flood events in an operational context. The resolution of this issue would requires the
576 development of an irrigation monitoring system, that would need intensive field surveys and mapping
577 but also the agreement of the local farmers that benefit from this system.

578

579 This study is a first step towards the development of operational flood forecasting systems in semi-arid
580 North Africa basins highly impacted by floods. Indeed, the evaluation of the most suitable satellite or
581 reanalysis products to estimate soil moisture for the monitoring of the basin saturation conditions
582 before floods is a necessary first step prior to implement flood warning systems based on rainfall and
583 soil moisture thresholds or coupled hydrometeorological modelling (Javelle et al., 2010; Norbiato et al.,
584 2008). One important aspect that should be addressed in further research aiming at developing a flood
585 forecasting system is the selection of soil moisture data based on the latency of these products. For
586 instance the ERA5 reanalysis is available within 5-days latency when ASCAT or SMOS satellite
587 products could be available with 3-hours latency. Prior to these developments, this type of evaluation
588 should be generalized in Morocco and other sites in North Africa where soil moisture measurements
589 are available, for the development of reliable flood forecasting systems using the outputs of
590 meteorological models in combination with the soil moisture state.

591

592 **Author Contributions:** E.E.; performed the analysis and wrote the paper, Y.T.; designed the analysis
593 and wrote the paper, C.M. and L.B.; designed the analysis and contributed to the paper, C.M.
594 performed the TC analysis, and M.S.; contributed to the paper

595

596 **Acknowledgments:** This research has been conducted in TREMA International Joint Laboratory
597 (<https://www.lmi-trema.ma/>) funded by the University Cadi Ayyad of Marrakech and the French IRD.



598 This work is a contribution to the HYdrological cycle in The Mediterranean EXperiment (HyMeX)
599 program, through INSU-MISTRALS support. The financial support provided by the ERASMUS+
600 mobility and the Centre National de la Recherche Scientifique et Technique (CNRS) are gratefully
601 acknowledged. Thanks are due to the hydrological basin agency Tensift (ABHT) and to the LMI
602 TREMA for providing the data. The Authors would like to thank Professor Khalid Chaouch for his
603 English revision.

604

605 **Conflicts of Interest:** The authors declare no conflict of interest.

606

607 **References**

608 Al-Yaari, A., Wigneron, J.-P., Ducharne, A., Kerr, Y. H., Wagner, W., De Lannoy, G., Reichle, R., Al
609 Bitar, A., Dorigo, W., Richaume, P. and Mialon, A.: Global-scale comparison of passive (SMOS) and
610 active (ASCAT) satellite based microwave soil moisture retrievals with soil moisture simulations
611 (MERRA-Land), *Remote Sens. Environ.*, 152, 614–626, doi:10.1016/J.RSE.2014.07.013, 2014.

612

613 El Alaoui El Fels, A., Bachnou, A. and Alaa, N.: Combination of GIS and mathematical modeling to
614 predict floods in semiarid areas: case of Rheraya watershed (Western High Atlas, Morocco), *Arab. J.*
615 *Geosci.*, 10(24), 554, doi:10.1007/s12517-017-3345-x, 2017.

616

617 Albergel, C., Calvet, J.-C., De Rosnay, P., Balsamo, G., Wagner, W., Hasenauer, S., Naeimi, V.,
618 Martin, E., Bazile, E., Bouyssel, F. and Mahfouf, J.-F.: Hydrology and Earth System Sciences Cross-
619 evaluation of modelled and remotely sensed surface soil moisture with in situ data in southwestern
620 France, *Hydrol. Earth Syst. Sci.*, 14, 2177–2191, doi:10.5194/hess-14-2177-2010, 2010.

621

622 Albergel, C., Dorigo, W., Balsamo, G., Muñoz-Sabater, J., de Rosnay, P., Isaksen, L., Brocca, L., de
623 Jeu, R. and Wagner, W.: Monitoring multi-decadal satellite earth observation of soil moisture products
624 through land surface reanalyses, *Remote Sens. Environ.*, 138, 77–89, doi:10.1016/J.RSE.2013.07.009,
625 2013.

626

627 Albergel, C., Dutra, E., Munier, S., Calvet, J.-C., Muñoz-Sabater, J., de Rosnay, P. and Balsamo, G.:
628 ERA-5 and ERA-Interim driven ISBA land surface model simulations: which one performs better?,
629 *Hydrol. Earth Syst. Sci.*, 22(6), 3515–3532, doi:10.5194/hess-22-3515-2018, 2018.

630

631 Anctil, F., Michel, C., Perrin, C. and Andréassian, V.: A soil moisture index as an auxiliary ANN
632 input for stream flow forecasting, *J. Hydrol.*, 286(1–4), 155–167,
633 doi:10.1016/J.JHYDROL.2003.09.006, 2004.

634



- 635 Bennani, O., Druon, E., Leone, F., Tramblay, Y. and Saidi, M. E. M.: A spatial and integrated flood
636 risk diagnosis, *Disaster Prev. Manag. An Int. J.*, DPM-12-2018-0379, doi:10.1108/DPM-12-2018-
637 0379, 2019.
- 638
- 639 Boudhar, A., Hanich, L., Boulet, G., Duchemin, B., Berjamy, B. and Chehbouni, A.: Evaluation of the
640 Snowmelt Runoff Model in the Moroccan High Atlas Mountains using two snow-cover estimates,
641 *Hydrol. Sci. J.*, 54(6), 1094–1113, doi:10.1623/hysj.54.6.1094, 2009.
- 642
- 643 Boumenni, H., Bachnou, A. and Alaa, N. E.: The rainfall-runoff model GR4J optimization of
644 parameter by genetic algorithms and Gauss-Newton method: application for the watershed Ourika
645 (High Atlas, Morocco), *Arab. J. Geosci.*, 10(15), 343, doi:10.1007/s12517-017-3086-x, 2017.
- 646
- 647 Brocca, L., Melone, F., Moramarco, T. and Morbidelli, R.: Antecedent wetness conditions based on
648 ERS scatterometer data, *J. Hydrol.*, doi:10.1016/j.jhydrol.2008.10.007, 2009a.
- 649
- 650 Brocca, L., Melone, F., Moramarco, T. and Morbidelli, R.: Soil moisture temporal stability over
651 experimental areas in Central Italy, *Geoderma*, doi:10.1016/j.geoderma.2008.11.004, 2009b.
- 652
- 653 Brocca, L., Melone, F., Moramarco, T. and Morbidelli, R.: Spatial-temporal variability of soil
654 moisture and its estimation across scales, *Water Resour. Res.*, doi:10.1029/2009WR008016, 2010.
- 655
- 656 Brocca, L., Hasenauer, S., Lacava, T., Melone, F., Moramarco, T., Wagner, W., Dorigo, W., Matgen,
657 P., Martínez-Fernández, J., Llorens, P., Latron, J., Martin, C. and Bittelli, M.: Soil moisture estimation
658 through ASCAT and AMSR-E sensors: An intercomparison and validation study across Europe,
659 *Remote Sens. Environ.*, doi:10.1016/j.rse.2011.08.003, 2011.
- 660
- 661 Brocca, L., Crow, W. T., Ciabatta, L., Massari, C., De Rosnay, P., Enenkel, M., Hahn, S., Amarnath,
662 G., Camici, S., Tarpanelli, A. and Wagner, W.: A Review of the Applications of ASCAT Soil
663 Moisture Products, *IEEE J. Sel. Top. Appl. Earth Obs. Remote Sens.*, 10(5), 2285–2306,
664 doi:10.1109/JSTARS.2017.2651140, 2017.
- 665
- 666 Chaponnière, A., Boulet, G., Chehbouni, A. and Aresmouk, M.: Understanding hydrological processes
667 with scarce data in a mountain environment, *Hydrol. Process.*, 22(12), 1908–1921,
668 doi:10.1002/hyp.6775, 2008.
- 669
- 670 Creutin, J.-D. and Borga, M.: Radar hydrology modifies the monitoring of flash-flood hazard, *Hydrol.*
671 *Process.*, 17(7), 1453–1456, doi:10.1002/hyp.5122, 2003.



672
673 Van doninck, J., Peters, J., Lievens, H., De Baets, B. and Verhoest, N. E. C.: Accounting for
674 seasonality in a soil moisture change detection algorithm for ASAR Wide Swath time series, *Hydrol.*
675 *Earth Syst. Sci.*, 16(3), 773–786, doi:10.5194/hess-16-773-2012, 2012.
676
677 Dorigo, W., de Jeu, R., Chung, D., Parinussa, R., Liu, Y., Wagner, W. and Fernández-Prieto, D.:
678 Evaluating global trends (1988-2010) in harmonized multi-satellite surface soil moisture, *Geophys.*
679 *Res. Lett.*, 39(18), doi:10.1029/2012GL052988, 2012.
680
681 Dorigo, W., Wagner, W., Albergel, C., Albrecht, F., Balsamo, G., Brocca, L., Chung, D., Ertl, M.,
682 Forkel, M., Gruber, A., Haas, E., Hamer, P. D., Hirschi, M., Ikonen, J., de Jeu, R., Kidd, R., Lahoz,
683 W., Liu, Y. Y., Miralles, D., Mistelbauer, T., Nicolai-Shaw, N., Parinussa, R., Pratola, C., Reimer, C.,
684 van der Schalie, R., Seneviratne, S. I., Smolander, T. and Lecomte, P.: ESA CCI Soil Moisture for
685 improved Earth system understanding: State-of-the art and future directions, *Remote Sens. Environ.*,
686 203, 185–215, doi:10.1016/j.rse.2017.07.001, 2017.
687
688 Dorigo, W. A., Gruber, A., De Jeu, R. A. M., Wagner, W., Stacke, T., Loew, A., Albergel, C., Brocca,
689 L., Chung, D., Parinussa, R. M. and Kidd, R.: Evaluation of the ESA CCI soil moisture product using
690 ground-based observations, , doi:10.1016/j.rse.2014.07.023, 2015.
691
692 Fernandez-Moran, R., Wigneron, J.-P., De Lannoy, G., Lopez-Baeza, E., Parrens, M., Mialon, A.,
693 Mahmoodi, A., Al-Yaari, A., Bircher, S., Al Bitar, A., Richaume, P. and Kerr, Y.: A new calibration
694 of the effective scattering albedo and soil roughness parameters in the SMOS SM retrieval algorithm,
695 *Int. J. Appl. Earth Obs. Geoinf.*, 62, 27–38, doi:10.1016/J.JAG.2017.05.013, 2017.
696
697 Gaume, E., Livet, M., Desbordes, M. and Villeneuve, J.-P.: Hydrological analysis of the river Aude,
698 France, flash flood on 12 and 13 November 1999, *J. Hydrol.*, 286(1–4), 135–154,
699 doi:10.1016/J.JHYDROL.2003.09.015, 2004.
700
701 Gruber, A., Dorigo, W. A., Crow, W. and Wagner, W.: Triple Collocation-Based Merging of Satellite
702 Soil Moisture Retrievals, *IEEE Trans. Geosci. Remote Sens.*, 55(12), 6780–6792,
703 doi:10.1109/TGRS.2017.2734070, 2017.
704
705 Gruber, A., Scanlon, T., Van Der Schalie, R., Wagner, W. and Dorigo, W.: Evolution of the ESA CCI
706 Soil Moisture climate data records and their underlying merging methodology, *Earth Syst. Sci. Data*,
707 11, 717–739, doi:10.5194/essd-11-717-2019, 2019.
708



- 709 Hargreaves, G. H. and Samani, Z. A.: Estimating Potential Evapotranspiration, *J. Irrig. Drain. Div.*,
710 108(3), 225–230, 1982.
- 711
- 712 Hwang, S. O., Park, J. and Kim, H. M.: Effect of hydrometeor species on very-short-range simulations
713 of precipitation using ERA5, *Atmos. Res.*, 218(December 2018), 245–256,
714 doi:10.1016/j.atmosres.2018.12.008, 2019.
- 715
- 716 Jackson, T. J., Cosh, M. H., Bindlish, R., Starks, P. J., Bosch, D. D., Seyfried, M., Goodrich, D. C.,
717 Moran, M. S. and Du, J.: Validation of advanced microwave scanning radiometer soil moisture
718 products, *IEEE Trans. Geosci. Remote Sens.*, 48(12), 4256–4272, doi:10.1109/TGRS.2010.2051035,
719 2010.
- 720
- 721 Jarlan, L., Khabba, S., Er-Raki, S., Le Page, M., Hanich, L., Fakir, Y., Merlin, O., Mangiarotti, S.,
722 Gascoin, S., Ezzahar, J., Kharrou, M. H., Berjamy, B., Saaïdi, A., Boudhar, A., Benkaddour, A.,
723 Laftouhi, N., Abaoui, J., Tavernier, A., Boulet, G., Simonneaux, V., Driouech, F., El Adnani, M., El
724 Fazziki, A., Amenzou, N., Raïbi, F., El Mandour, A., Ibouh, H., Le Dantec, V., Habets, F., Tramblay,
725 Y., Mougnot, B., Leblanc, M., El Faïz, M., Drapeau, L., Coudert, B., Hagolle, O., Filali, N., Belaqqiz,
726 S., Marchane, A., Szczypta, C., Toumi, J., Diarra, A., Aouade, G., Hajhouji, Y., Nassah, H., Bigeard,
727 G., Chirouze, J., Boukhari, K., Abourida, A., Richard, B., Fanise, P., Kasbani, M., Chakir, A., Zribi,
728 M., Marah, H., Naimi, A., Mokssit, A., Kerr, Y. and Escadafal, R.: Remote Sensing of Water
729 Resources in Semi-Arid Mediterranean Areas: the joint international laboratory TREMA, *Int. J.*
730 *Remote Sens.*, 36(19–20), 4879–4917, doi:10.1080/01431161.2015.1093198, 2015.
- 731
- 732 Javelle, P., Fouchier, C., Arnaud, P. and Lavabre, J.: Flash flood warning at ungauged locations using
733 radar rainfall and antecedent soil moisture estimations, *J. Hydrol.*, doi:10.1016/j.jhydrol.2010.03.032,
734 2010.
- 735
- 736 Jiang, D. and Wang, K.: The role of satellite-based remote sensing in improving simulated streamflow:
737 A review, *Water (Switzerland)*, 11(8), doi:10.3390/w11081615, 2019.
- 738
- 739 Kerr, Y. H., Waldteufel, P., Wigneron, J.-P., Martinuzzi, J.-M., Font, J. and Berger, M.: Soil Moisture
740 Retrieval from Space: The Soil Moisture and Ocean Salinity (SMOS) Mission. 2001.
- 741
- 742 Kerr, Y. H., Waldteufel, P., Richaume, P., Wigneron, J. P., Ferrazzoli, P., Mahmoodi, A., Al Bitar, A.,
743 Cabot, F., Gruhier, C., Juglea, S. E., Leroux, D., Mialon, A. and Delwart, S.: The SMOS Soil Moisture
744 Retrieval Algorithm, *IEEE Trans. Geosci. Remote Sens.*, 50(5), 1384–1403,
745 doi:10.1109/TGRS.2012.2184548, 2012.



- 746
- 747 Khabba, S., Jarlan, L., Er-Raki, S., Le Page, M., Ezzahar, J., Boulet, G., Simonneaux, V., Kharrou, M.
748 H., Hanich, L. and Chehbouni, G.: The SudMed Program and the Joint International Laboratory
749 TREMA: A Decade of Water Transfer Study in the Soil-plant-atmosphere System over Irrigated Crops
750 in Semi-arid Area, *Procedia Environ. Sci.*, 19, 524–533, doi:10.1016/J.PROENV.2013.06.059, 2013.
- 751
- 752 El Khalki, E. M., Trambly, Y., El Mehdi Saidi, M., Bouvier, C., Hanich, L., Benrhanem, M. and
753 Alaouri, M.: Comparison of modeling approaches for flood forecasting in the High Atlas Mountains of
754 Morocco, *Arab. J. Geosci.*, 11(15), doi:10.1007/s12517-018-3752-7, 2018.
- 755
- 756 Koster, R. D., Guo, Z., Yang, R., Dirmeyer, P. A., Mitchell, K., Puma, M. J., Koster, R. D., Guo, Z.,
757 Yang, R., Dirmeyer, P. A., Mitchell, K. and Puma, M. J.: On the Nature of Soil Moisture in Land
758 Surface Models, *J. Clim.*, 22(16), 4322–4335, doi:10.1175/2009JCLI2832.1, 2009.
- 759
- 760 Liu, Y. Y., Parinussa, R. M., Dorigo, W. A., De Jeu, R. A. M., Wagner, W., M. Van Dijk, A. I. J.,
761 McCabe, M. F. and Evans, J. P.: Developing an improved soil moisture dataset by blending passive
762 and active microwave satellite-based retrievals, *Hydrol. Earth Syst. Sci.*, doi:10.5194/hess-15-425-
763 2011, 2011.
- 764
- 765 Loew, A. and Mauser, W.: On the disaggregation of passive microwave soil moisture data using A
766 Priori knowledge of temporally persistent soil moisture fields, *IEEE Trans. Geosci. Remote Sens.*,
767 46(3), 819–834, doi:10.1109/TGRS.2007.914800, 2008.
- 768
- 769 Loew, A. and Schlenz, F.: A dynamic approach for evaluating coarse scale satellite soil moisture
770 products, *Hydrol. Earth Syst. Sci.*, 15(1), 75–90, doi:10.5194/hess-15-75-2011, 2011.
- 771
- 772 Ma, H., Zeng, J., Chen, N., Zhang, X., Cosh, M. H. and Wang, W.: Satellite surface soil moisture from
773 SMAP, SMOS, AMSR2 and ESA CCI: A comprehensive assessment using global ground-based
774 observations, *Remote Sens. Environ.*, 231, doi:10.1016/j.rse.2019.111215, 2019.
- 775
- 776 Mahto, S. S. and Mishra, V.: Does ERA-5 Outperform Other Reanalysis Products for Hydrologic
777 Applications in India?, *J. Geophys. Res. Atmos.*, 124(16), 9423–9441, doi:10.1029/2019JD031155,
778 2019.
- 779
- 780 Marchandise, A. and Viel, C.: Utilisation des indices d’humidité de la chaîne Safran-Isba-Modcou de
781 Météo-France pour la vigilance et la prévision opérationnelle des crues, *La Houille Blanche*,
782 doi:10.1051/lhb/2009075, 2010.



- 783
- 784 Martínez-Fernández, J. and Ceballos, A.: Mean soil moisture estimation using temporal stability
785 analysis, *J. Hydrol.*, 312(1–4), 28–38, doi:10.1016/j.jhydrol.2005.02.007, 2005.
- 786
- 787 Massari, C., Brocca, L., Moramarco, T., Tramblay, Y. and Didon Lescot, J.-F.: Potential of soil
788 moisture observations in flood modelling: estimating initial conditions and correcting rainfall, *Adv.*
789 *Water Resour.*, 74, 44–53, doi:10.1016/j.advwatres.2014.08.004, 2014.
- 790
- 791 Massari, C., Brocca, L., Ciabatta, L., Moramarco, T., Gabellani, S., Albergel, C., De Rosnay, P., Puca,
792 S. and Wagner, W.: The Use of H-SAF Soil Moisture Products for Operational Hydrology: Flood
793 Modelling over Italy, *Hydrology*, 2(1), 2–22, doi:10.3390/hydrology2010002, 2015.
- 794
- 795 Merheb, M., Moussa, R., Abdallah, C., Colin, F., Perrin, C. and Baghdadi, N.: Hydrological response
796 characteristics of Mediterranean catchments at different time scales: a meta-analysis, ,
797 doi:10.1080/02626667.2016.1140174, 2016.
- 798
- 799 Miliani, F., Ravazzani, G. and Mancini, M.: Adaptation of Precipitation Index for the Estimation of
800 Antecedent Moisture Condition in Large Mountainous Basins, *J. Hydrol. Eng.*, 16(3), 218–227,
801 doi:10.1061/(ASCE)HE.1943-5584.0000307, 2011.
- 802
- 803 Miralles, D. G., Crow, W. T. and Cosh, M. H.: Estimating Spatial Sampling Errors in Coarse-Scale
804 Soil Moisture Estimates Derived from Point-Scale Observations, *J. Hydrometeorol.*, 11(6), 1423–
805 1429, doi:10.1175/2010JHM1285.1, 2010.
- 806
- 807 Nash, J. E. and Sutcliffe, J. V.: River flow forecasting through conceptual models part I — A
808 discussion of principles, *J. Hydrol.*, 10(3), 282–290, doi:10.1016/0022-1694(70)90255-6, 1970.
- 809
- 810 Norbiato, D., Borga, M., Degli Esposti, S., Anquetin, S. and Gaume, E.: Flash flood warning based on
811 rainfall thresholds and soil moisture conditions: An assessment for gauged and ungauged basins, *J.*
812 *Hydrol.*, doi:10.1016/j.jhydrol.2008.08.023, 2008.
- 813
- 814 Ochsner, T. E., Cosh, M. H., Cuenca, R. H., Dorigo, W. A., Draper, C. S., Hagimoto, Y., Kerr, Y. H.,
815 Njoku, E. G., Small, E. E., Zreda, M. and Larson, K. M.: State of the Art in Large-Scale Soil Moisture
816 Monitoring, *Soil Sci. Soc. Am. J.*, 77(6), 1888, doi:10.2136/sssaj2013.03.0093, 2013.
- 817
- 818 Olauson, J.: ERA5: The new champion of wind power modelling?, *Renew. Energy*, 126, 322–331,
819 doi:10.1016/j.renene.2018.03.056, 2018.



- 820
- 821 Oudin, L., Michel, C. and Anctil, F.: Which potential evapotranspiration input for a lumped rainfall-
822 runoff model?: Part 1—Can rainfall-runoff models effectively handle detailed potential
823 evapotranspiration inputs?, *J. Hydrol.*, 303(1–4), 275–289, doi:10.1016/J.JHYDROL.2004.08.025,
824 2005.
- 825
- 826 Pérennès, J. J.: L'eau et les hommes au Maghreb. Contribution à une politique de l'eau en
827 Méditerranée, *Rev. Tiers Monde*, 35(137), 231–232, 1994.
- 828
- 829 Saidi, M. E. M., Daoudi, L., Aresmouk, M. E. H. and Blali, A.: Rôle du milieu physique dans
830 l'amplification des crues en milieu montagnard: exemple de la crue du 17 août 1995 dans la vallée de
831 l'Ourika (Haut-Atlas, Maroc), *Sécheresse*, v. 14(2), 2003
- 832
- 833 Schulte, R. P. O., Diamond, J., Finkele, K., Holden, N. M. and Breteron, A. J.: Predicting the Soil
834 Moisture Conditions of Irish Grasslands, *Irish J. Agric. Food Res.*, 44, 95–110, doi:10.2307/25562535,
835 2005.
- 836
- 837 Trambly, Y., Bouvier, C., Crespy, A. and Marchandise, A.: Improvement of flash flood modelling
838 using spatial patterns of rainfall : a case study in southern France, , 2(October), 172–178, 2010.
- 839
- 840 Trambly, Y., Bouvier, C., Ayrat, P. A. and Marchandise, A.: Impact of rainfall spatial distribution on
841 rainfall-runoff modelling efficiency and initial soil moisture conditions estimation, *Nat. Hazards Earth*
842 *Syst. Sci.*, doi:10.5194/nhess-11-157-2011, 2011.
- 843
- 844 Trambly, Y., Bouaicha, R., Brocca, L., Dorigo, W., Bouvier, C., Camici, S. and Servat, E.:
845 Estimation of antecedent wetness conditions for flood modelling in northern Morocco, *Hydrol. Earth*
846 *Syst. Sci.*, 16(11), 4375–4386, doi:10.5194/hess-16-4375-2012, 2012.
- 847
- 848 Tuttle, S. E. and Salvucci, G. D.: A new approach for validating satellite estimates of soil moisture
849 using large-scale precipitation: Comparing AMSR-E products, *Remote Sens. Environ.*, 142, 207–222,
850 doi:10.1016/j.rse.2013.12.002, 2014.
- 851
- 852 US Army Corps of Engineers: Hydrologic Modelling System HEC-HMS., 2015.
- 853
- 854 Vachaud, G., Passerat De Silans, A., Balabanis, P. and Vauclin, M.: Temporal stability of spatially
855 measured soil water probability density function., *Soil Sci. Soc. Am. J.*, 49(4), 822–828,
856 doi:10.2136/sssaj1985.03615995004900040006x, 1985.



857
858 Vinet, F., El Mehdi Saidi, M., Douvinet, J., Fehri, N., Nasrallah, W., Menad, W. and Mellas, S.: Sub-
859 chapter 3.4.1. Urbanization and land use as a driver of flood risk, in *The Mediterranean region under*
860 *climate change*, pp. 563–575, IRD Éditions., 2016.

861
862 Wagner, W., Pathe, C., Doubkova, M., Sabel, D., Bartsch, A., Hasenauer, S., Blöschl, G., Scipal, K.,
863 Martínez-Fernández, J. and Löw, A.: Temporal Stability of Soil Moisture and Radar Backscatter
864 Observed by the Advanced Synthetic Aperture Radar (ASAR), *Sensors*, 8(2), 1174–1197,
865 doi:10.3390/s80201174, 2008.

866
867 Wagner, W., Hahn, S., Kidd, R., Melzer, T., Bartalis, Z., Hasenauer, S., Figa-Saldaña, J., de Rosnay,
868 P., Jann, A., Schneider, S., Komma, J., Kubu, G., Brugger, K., Aubrecht, C., Züger, J., Gangkofner,
869 U., Kienberger, S., Brocca, L., Wang, Y., Blöschl, G., Eitzinger, J. and Steinnocher, K.: The ASCAT
870 Soil Moisture Product: A Review of its Specifications, Validation Results, and Emerging
871 Applications, *Meteorol. Zeitschrift*, 22(1), 5–33, doi:10.1127/0941-2948/2013/0399, 2013.

872
873 Western, A. W. and Blöschl, G.: On the spatial scaling of soil moisture, *Journal of Hydrology*, 217(3),
874 203–224, doi: 10.1016/S0022-1694(98)00232-7, 1999.

875
876 Wigneron, J.-P., Kerr, Y., Waldteufel, P., Saleh, K., Escorihuela, M.-J., Richaume, P., Ferrazzoli, P.,
877 de Rosnay, P., Gurney, R., Calvet, J.-C., Grant, J. P., Guglielmetti, M., Hornbuckle, B., Mätzler, C.,
878 Pellarin, T. and Schwank, M.: L-band Microwave Emission of the Biosphere (L-MEB) Model:
879 Description and calibration against experimental data sets over crop fields, *Remote Sens. Environ.*,
880 107(4), 639–655, doi:10.1016/J.RSE.2006.10.014, 2007.

881
882 Zema, Demetrio I. Zema, D.A.; Labate, A.; Martino, D.; Zimbone, S.M. Comparing Different
883 Infiltration Methods of the HEC-HMS Model: The Case Study of the Mésima Torrent (Southern
884 Italy). *L. Degrad. Dev.* 2017, 28, 294–308. Antonio, Labate, A., Martino, D. and Zimbone, S. M.:
885 Comparing Different Infiltration Methods of the HEC-HMS Model: The Case Study of the Mésima
886 Torrent (Southern Italy), *L. Degrad. Dev.*, 28(1), 294–308, doi:10.1002/ldr.2591, 2017.

887
888 Zeng, J., Li, Z., Chen, Q., Bi, H., Qiu, J. and Zou, P.: Evaluation of remotely sensed and reanalysis
889 soil moisture products over the Tibetan Plateau using in-situ observations, *Remote Sens. Environ.*,
890 163, 91–110, doi:10.1016/j.rse.2015.03.008, 2015.

891
892
893



894
 895
 896
 897
 898
 899
 900
 901
 902
 903
 904
 905
 906
 907
 908
 909
 910
 911
 912
 913
 914
 915

TABLES

Table 1: Characteristics of the selected flood events.

Rheraya				
	Max Discharge [m ³ /s]	Volume [10 ³ m ³]	Precipitation Volume [10³ m³]	Runoff Coefficient [%]
23/01/2014	17.1	459.2	2749.5	16.7
29/01/2014	39.7	602.8	2632.5	22.9
10/02/2014	19.2	543.2	2904.7	18.7
11/03/2014	19	557	1633.5	34.1
21/04/2014	38.2	1070	5431.5	19.7
21/09/2014	24.4	440.6	3363.8	13.1
05/11/2014	46.5	1027	5737.5	17.9
09/11/2014	42.2	869.3	4575.2	19
22/11/2014	99.5	3868.9	17586	22
28/11/2014	76.4	3797.2	11940.8	31.8
Issyl				
25/03/2011	63.8	385.28	27520	1.4



03/04/2011	16.6	550.656	30592	1.8
29/04/2011	19.7	246.4	11200	2.2
02/05/2011	17.1	303.36	10112	3.0
16/05/2011	45.8	361.12	9760	3.7
19/05/2011	27.6	315.392	7168	4.4
06/06/2011	18.3	212.352	5056	4.2
02/04/2012	16.8	216.576	18048	1.2
05/04/2012	20	543.744	7552	7.2
28/09/2012	22.7	126.72	7040	1.8
05/04/2013	15.4	365.376	16608	2.2
28/11/2014	37.2	489.6	28800	1.7
25/03/2015	16.2	767.424	18272	4.2

916

917

918

919

920

921

Table 2: Results of correlation analysis between soil moisture data and in-situ measurements and SMA model (significant correlations are represented in bold)

922

923

		Winter	Spring	Summer	Fall
Rheraya					
In-situ	SMA A=8mm	0.82	0.83	0.67	0.75
	In-situ	0.47	-0.03	0.18	0.70
ASCAT	SMA A=8mm	0.32	0.09	0.54	0.65
	In-situ	0.01	0.68	0.61	0.16
SMOS	SMA A=8mm	-0.09	0.75	0.58	0.54
	In-situ	0.80	0.68	0.45	0.85
SMOS-IC	SMA A=8mm	0.80	0.72	0.62	0.57
	In-situ	0.12	0.28	0.41	0.60
ESACCI	SMA A=8mm	0.15	0.30	0.67	0.51
	In-situ	0.74	0.73	0.04	0.73
ERA5	SMA A=8mm	0.86	0.76	0.54	0.65
	In-situ	0.43	0.47	0.34	0.61
Mean	SMA A=8mm	0.41	0.52	0.59	0.58
	Issyl				
ASCAT	SMA A=30mm	0.77	0.86	0.70	0.90
SMOS	SMA A=30mm	0.39	0.76	0.47	0.74



SMOS-IC		0.85	0.81	0.56	0.93
ESACCI		0.70	0.89	0.77	0.89
ERA5		0.88	0.82	0.70	0.88
Mean	SMA A=30mm	0.72	0.83	0.64	0.87

924

925

926 **Table 3: Signal to noise ratio for Rheraya and Issyl basins. The SNT = 0 : Error variance, SNR > 3 Signal**
 927 **variance double the noise variance (very good) and SNR < 3 Signal variance half noise variance (not**
 928 **good).**

	ASCAT	SMOS	SMOS-IC	ERA5	SMA
Rheraya	-5.55		7.54		-1.99
	-6.16	4.31		1.16	-1.10
Issyl	4.23	1.90		2.33	5.03
	4.28		8.12	2.33	4.99

929

930

931

932

933

934

935 **Table 4: Calibration results of SCS-CN model, S is the potential maximum soil moisture retention,**
 936 **BIAS_Q is the difference between the observed and calibrated peak discharge of the event, BIAS_V is**
 937 **the difference between the observed and calibrated volume of the event.**

Rheraya					Issyl				
Events	S[mm]	Ns	BIAS_Q [%]	BIAS_V [%]	Events	S[mm]	Ns	BIAS_Q [%]	BIAS_V [%]
23/01/2014	19.1	-0.58	1.18	-5.76	25/03/2011	679.8	0,83	29,94	-13,5
29/01/2014	24.5	0.87	6.43	29.14	03/04/2011	730.5	0,02	-12,05	27,93
10/02/2014	34.6	0.71	-4	2.85	29/04/2011	218.1	0,83	0	10,36
11/03/2014	9.5	0.61	-17.39	2.57	02/05/2011	113	0,91	-0,58	44,39
21/04/2014	55.8	0.73	6.41	2.3	16/05/2011	176.5	0,61	17,69	-26,31
21/09/2014	34.6	0.77	27.08	-6.87	19/05/2011	136.7	0,87	1,09	9,64
05/11/2014	39.6	0.97	15.38	0.88	06/06/2011	108.8	0,75	0	-5,38
09/11/2014	40.7	0.83	6.3	-0.32	02/04/2012	440.3	0,56	0	15,26
22/11/2014	43.1	0.78	-5.06	2.38	05/04/2012	125.1	0,56	13,5	-1,91
28/11/2014	71.6	0.97	3.66	-6.22	28/09/2012	159.7	0,11	32,16	23,41
					05/04/2013	388.2	0,9	6,49	-4,16



				28/11/2014	254	0,74	1,88	0,71
				25/03/2015	356.6	0,89	0	12,32
Mean	0.67	4	2.09	Mean		0,66	6,93	7,14
Median	0.77	4.98	1.59	Median		0,75	1,09	9,64

938
 939
 940
 941
 942
 943
 944
 945
 946
 947
 948
 949
 950

951 **Table 5: Correlation between soil moisture products and the S parameter of the SCS-CN**
 952 **hydrological model**

	Rheraya		Issyl	
	S	Number of events	S	Number of events
In-situ [Daily]	-0.71	8	-	-
In-situ [Hourly]	-0.83	8	-	-
SMA A=8mm	-0.32	10	-	-
SMA A=30mm	0.02	10	-0.69	13
ASCAT	-0.55	10	-0,29	13
ESA-CCI	-0,29	8	-0.66	11
SMOS	0.12	6	-0,59	6
SMOS-IC	-0.81	10	-0.34	13
ERA5 [Daily]	-0.46	10	-0.37	13
ERA5 [Hourly]	-0.80	10	-0.63	13

953
 954
 955



956 **Table 6: Performance of the SCS-CN model in term of Nash Coefficient for the Rheraya and Issyl events,**
 957 **using the daily or hourly time steps for the different soil moisture products.**
 958

	Daily						Hourly		
	ASCAT	ESA-CCI	SMOS	SMOS-IC	ERA5	In-situ	SMA 30mm	ERA5	In-situ
RHERAYA									
Min	-0.15	-	-	-0.04	-0.73	-1.88	-	-0.01	0.15
Mean	0.48	-	-	0.58	0.45	0.25	-	0.64	0.54
Median	0.57	-	-	0.63	0.66	0.49	-	0.73	0.61
Max	0.85	-	-	0.84	0.82	0.83	-	0.81	0.71
ISSYL									
Min	-	-56041	-	-	-	-	-96.08	-114.6	-
Mean	-	-14138.2	1938.07	-	-	-	-24.77	-16.74	-
Median	-	-254.85	-1.8	-	-	-	-2.46	-0.85	-
Max	-	-2.10	-0.52	-	-	-	-0.78	0.83	-

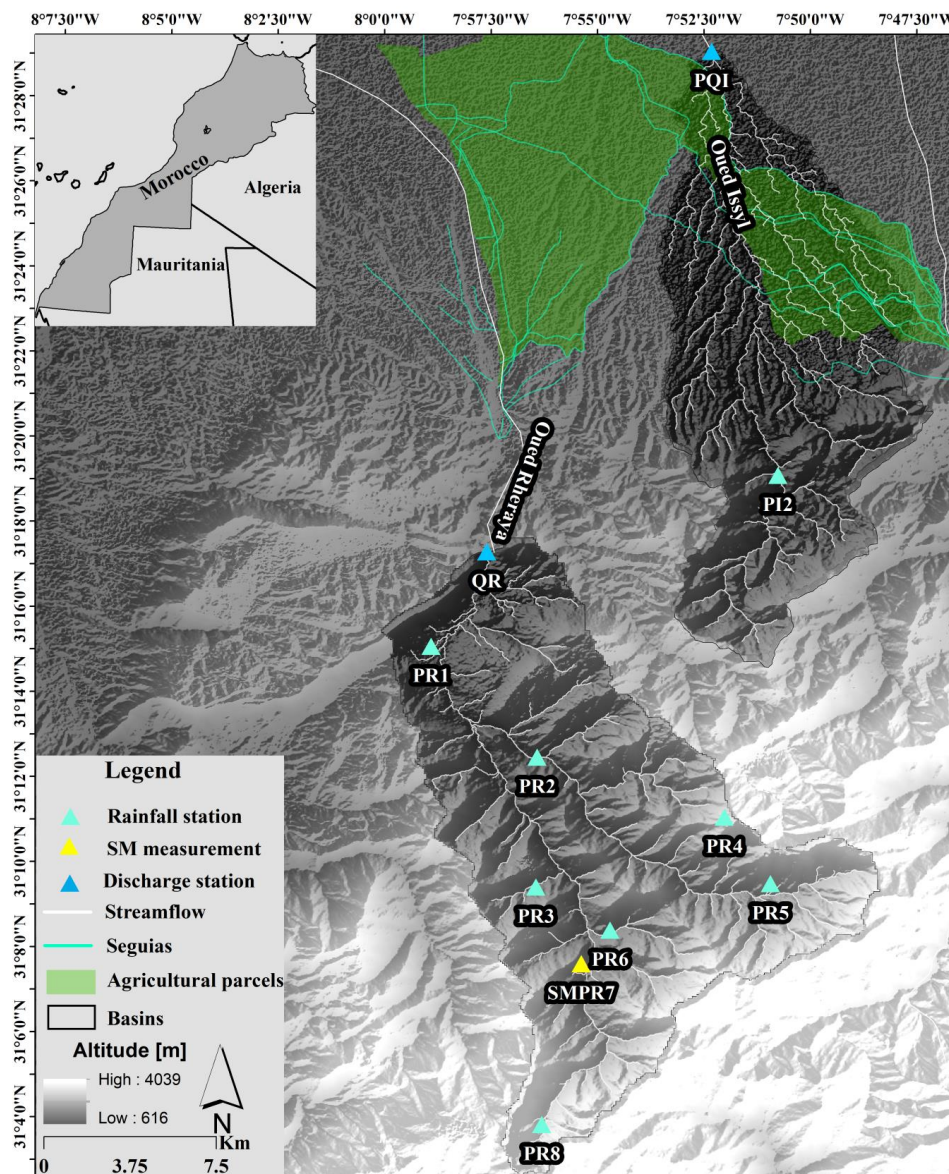
959
 960
 961
 962
 963
 964
 965
 966
 967
 968
 969
 970
 971
 972
 973
 974
 975
 976
 977
 978
 979



980 **FIGURES**

981

982



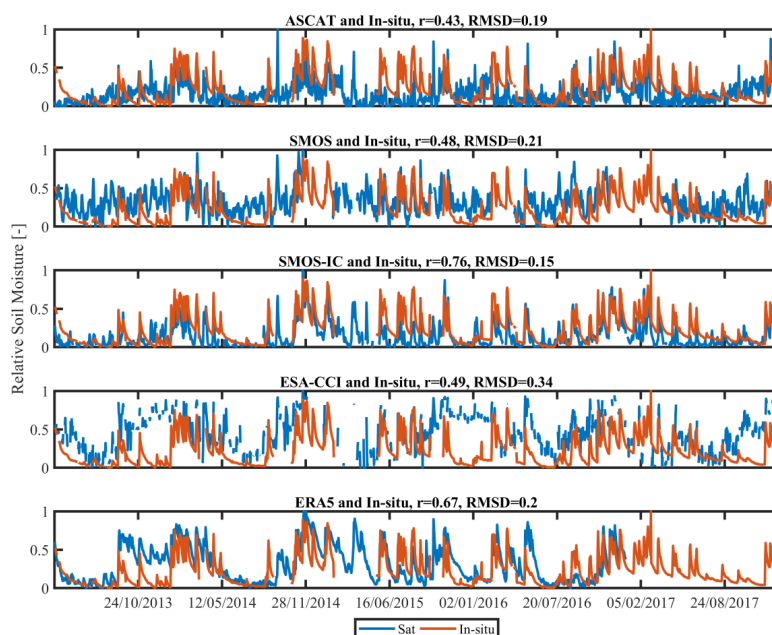
983

984 **Figure 1: Location of Rheraya and Issyl basins, the seguias network, the agricultural parcels and the**
985 **hydro-meteorological network – PR: Rainfall station in Rheraya, SMPR: Soil moisture measurement+**
986 **Rainfall station in Rheraya, PQ1: Rainfall and discharge station in Issyl, QR: Discharge station in**
987 **Rheraya.**

988



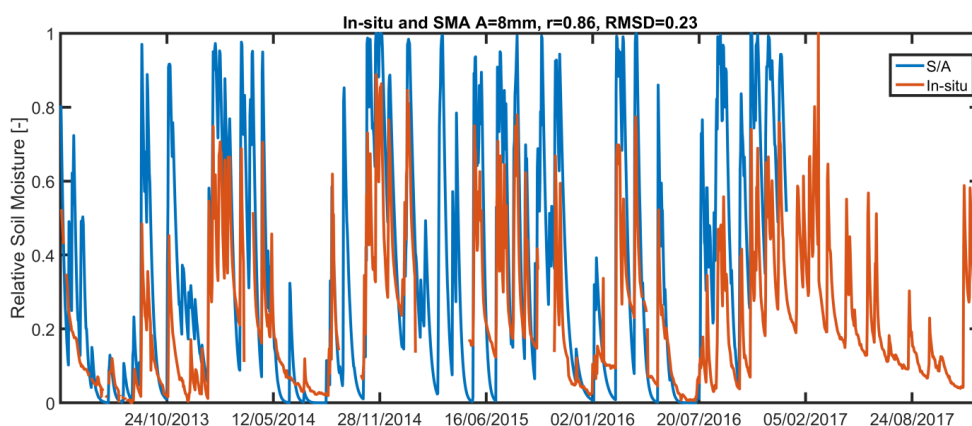
989



990

991 **Figure 2: Correlation between measurements of soil moisture (5cm depth) and different products of soil**
992 **moisture (Rheraya basin).**

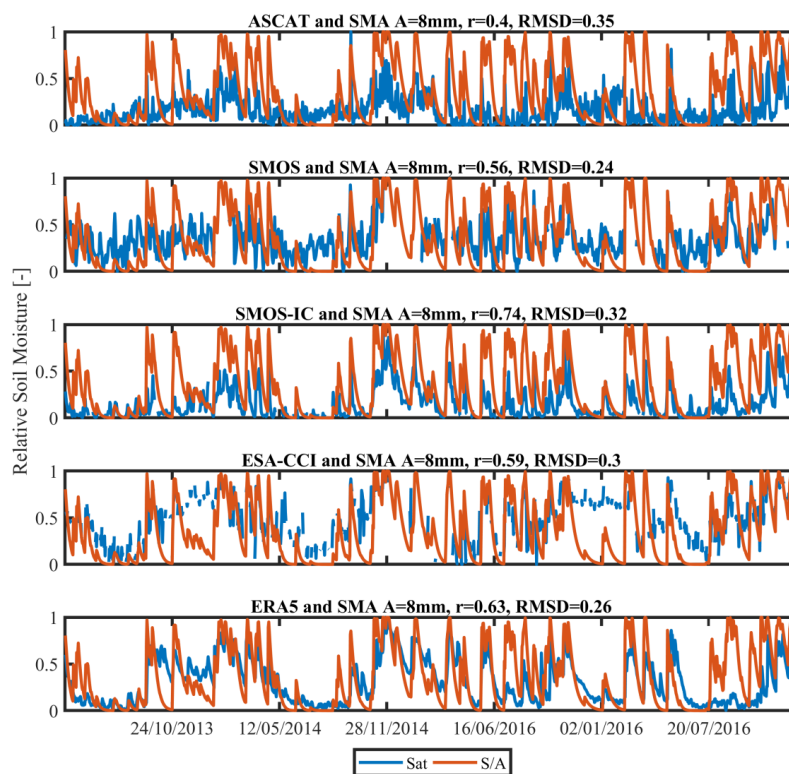
993



994

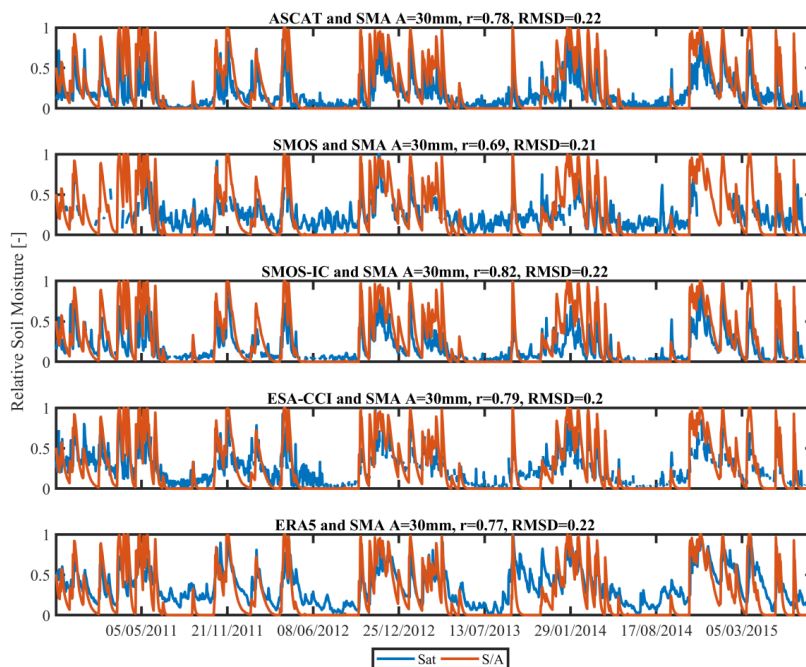
995 **Figure 3: Relationship between S/A and observed soil moisture data between 08/04/2013 and 31/12/2016**
996 **for different values of A (Rheraya basin).**

997



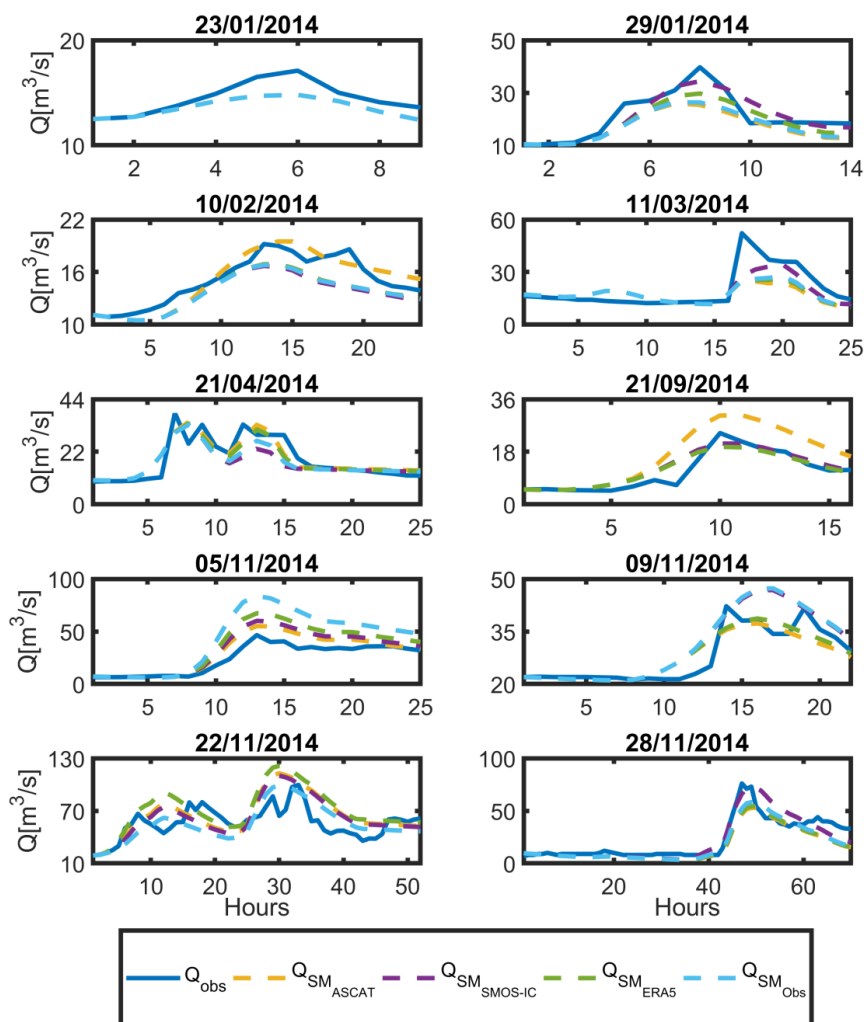
998

999 **Figure 4: Relationship between satellite products of soil moisture and ERA5 with and SMA outputs**
1000 **between 08/04/2013 and 31/12/2016 over the Rheraya basin.**



1001
1002
1003
1004

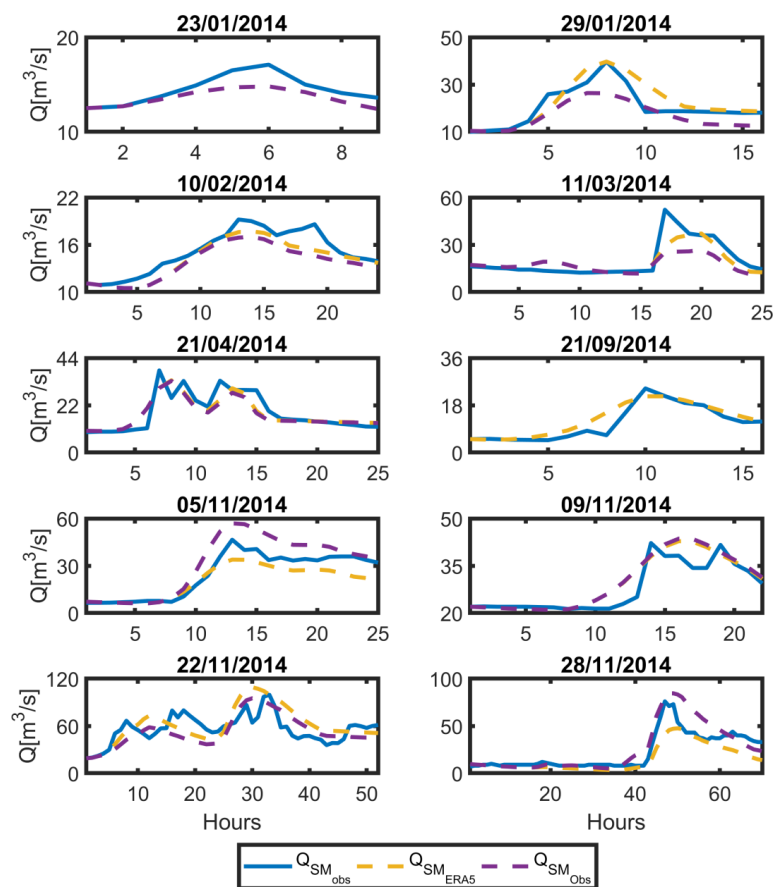
Figure 5: Relationship between Satellite products of soil moisture and SMA outputs for A=30mm between 18/10/2010 and 20/08/2015 in the Issyl basin



1005

1006 **Figure 6: Validation results of flood events simulated for the Rheraya using different soil moisture**
 1007 **products with a daily time step. The observed hydrograph (Q_{obs}) is compared to the simulated**
 1008 **hydrographs using ASCAT, SMOS-IC, ERA5 and in situ data.**

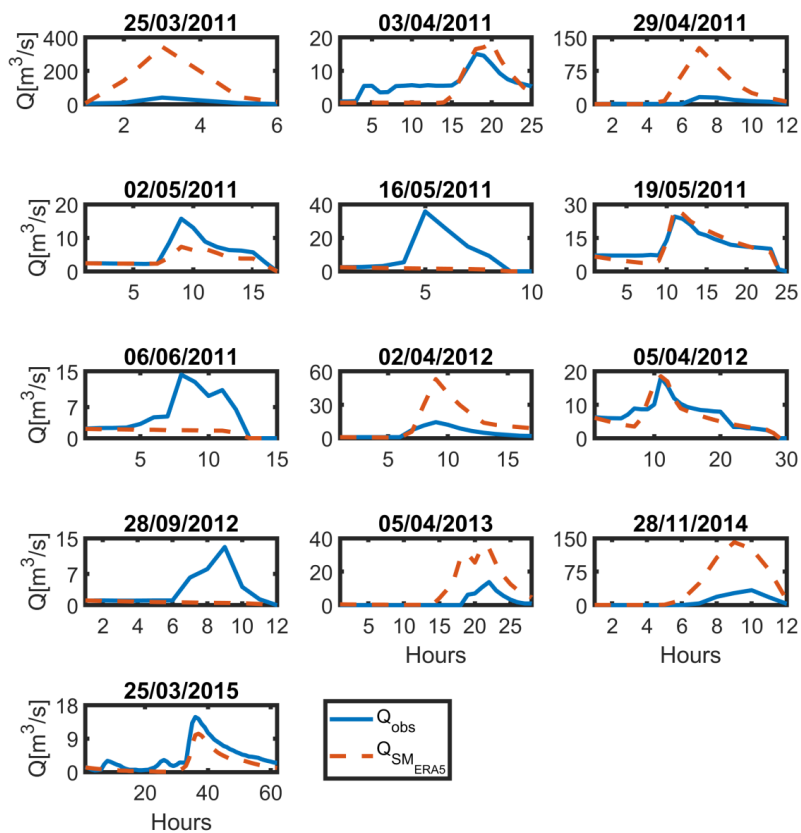
1009



1010

1011 **Figure 7: Validation of the flood events simulated for the Rheraya using ERA5 and in situ soil moisture**
1012 **with hourly time step.**

1013



1014

1015 **Figure 8: Validation result of flood events for the Issyl using ERA5 with hourly time step**

1016

1017